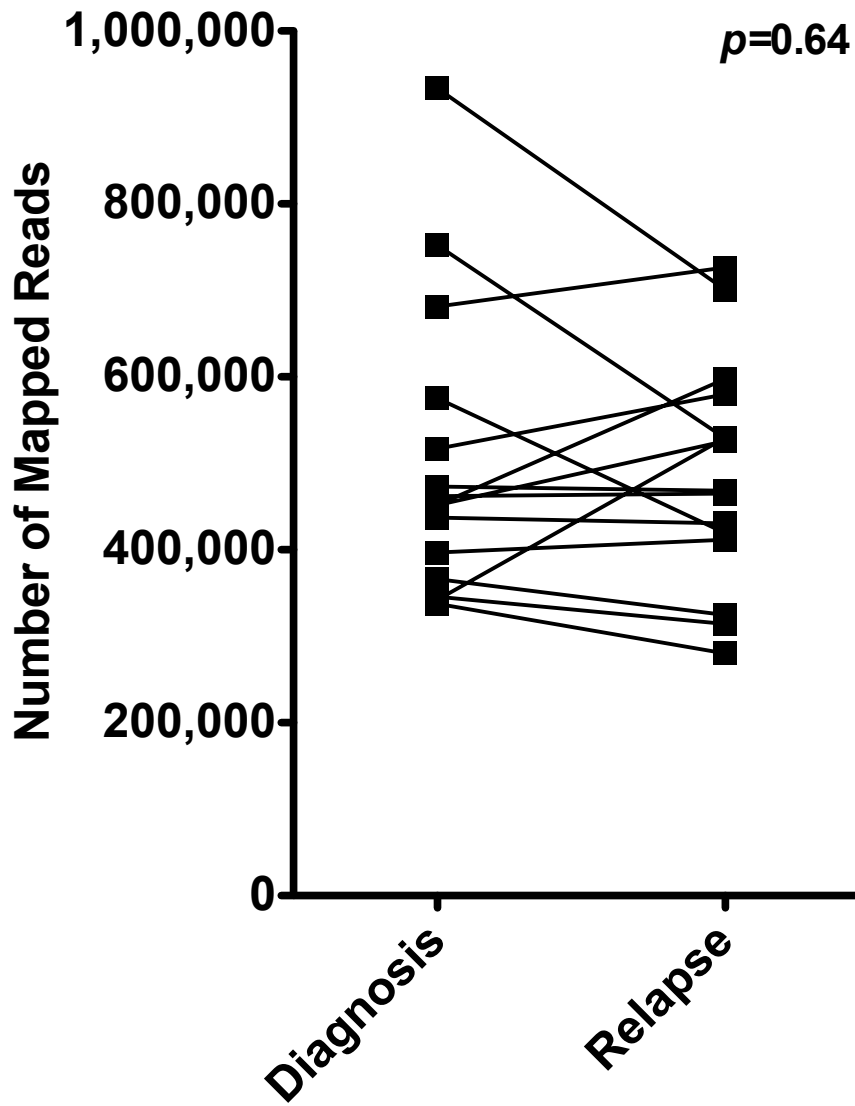
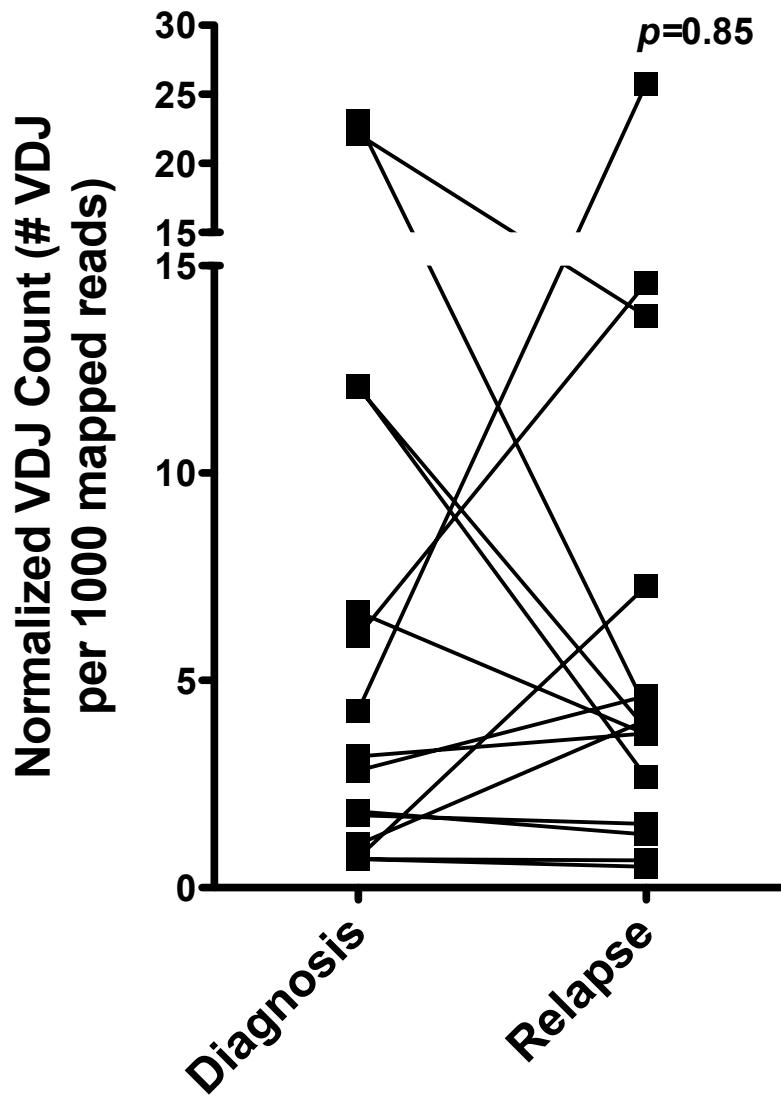


Supplementary Figure 1



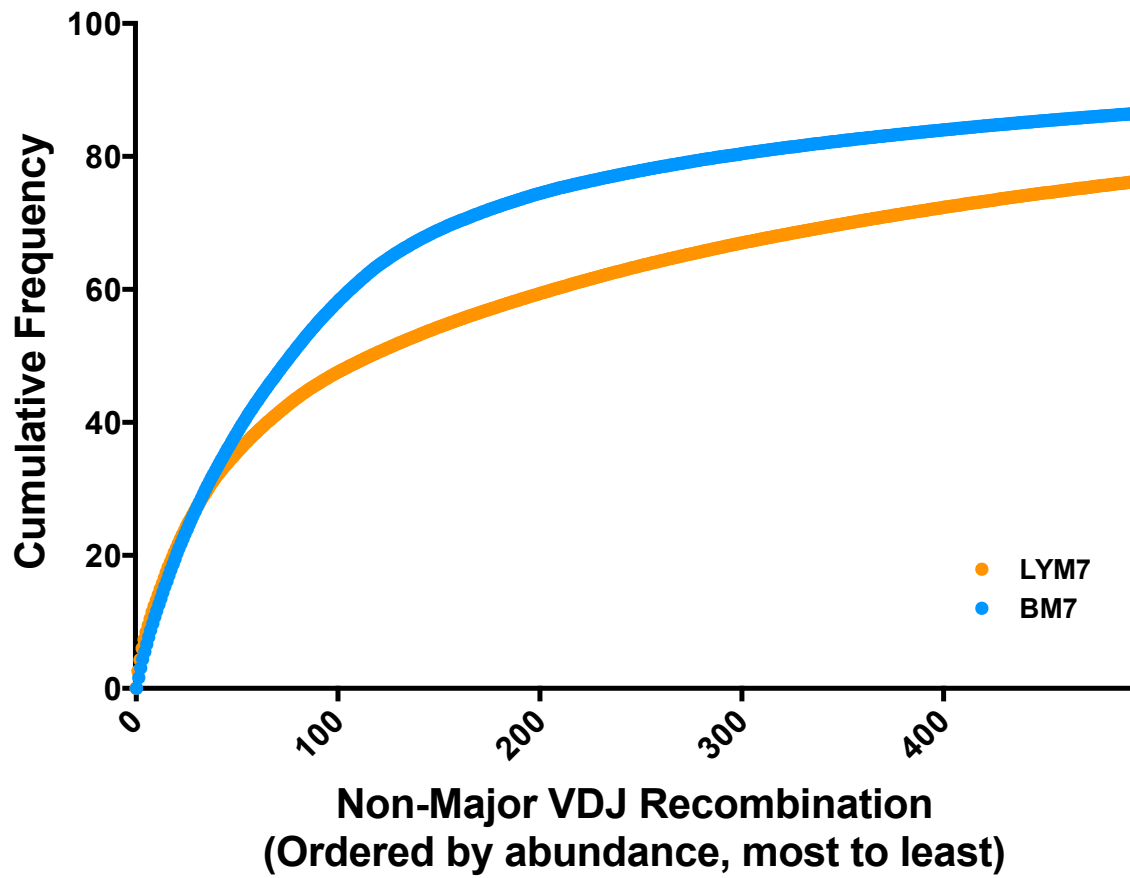
Supplementary Figure 1: Aligned reads number for each sample. Each dot represents one sample pair. The number of the aligned reads for the diagnosis sample of the pair was shown on the x-axis, and the number for the aligned reads for the relapse sample for the pair was shown on the y-axis.

Supplementary Figure 2



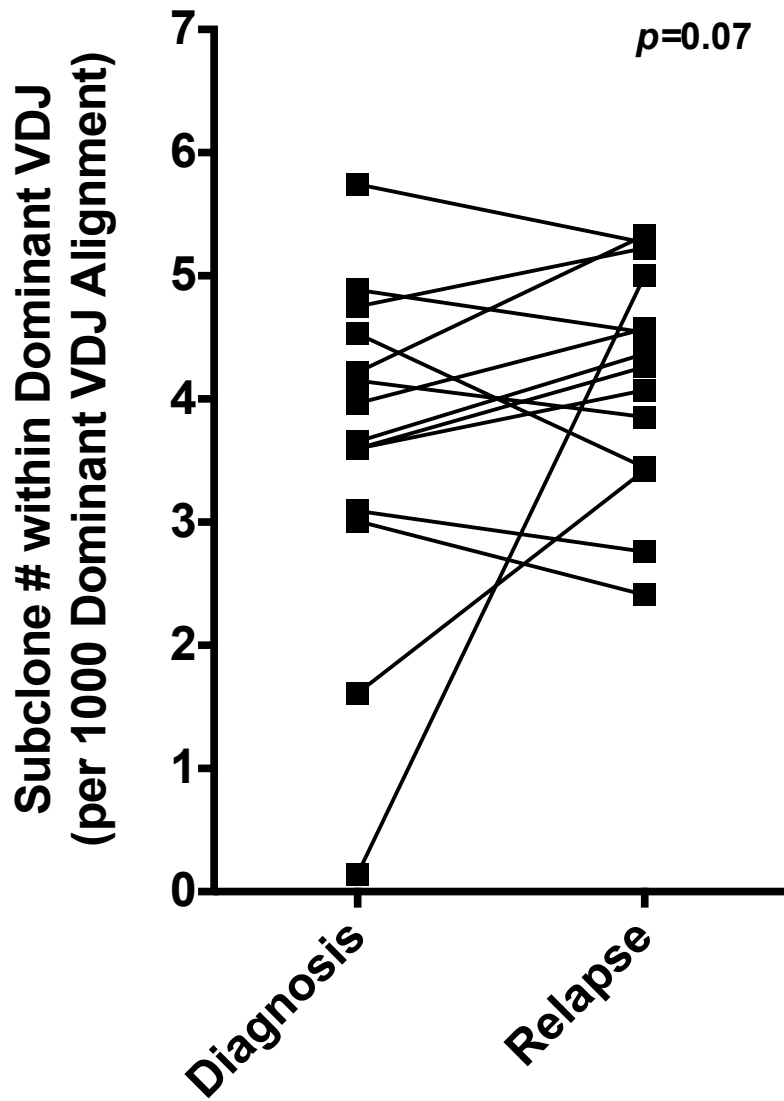
Supplementary Figure 2: Normalized VDJ counts (per 1000 mapped reads) of each sample.

Supplementary Figure 3



Supplementary Figure 3: Cumulative frequency of non-major VDJ rearrangements in a pair of bone marrow and lymphoma samples.

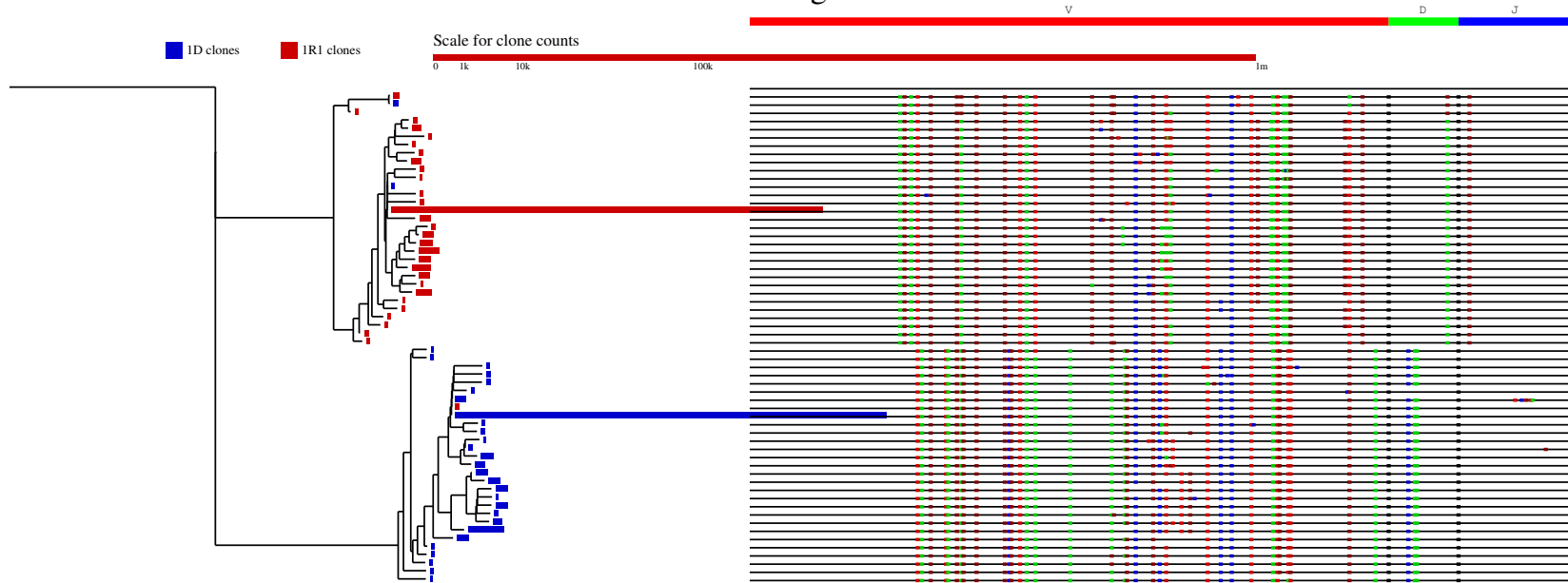
Supplementary Figure 4



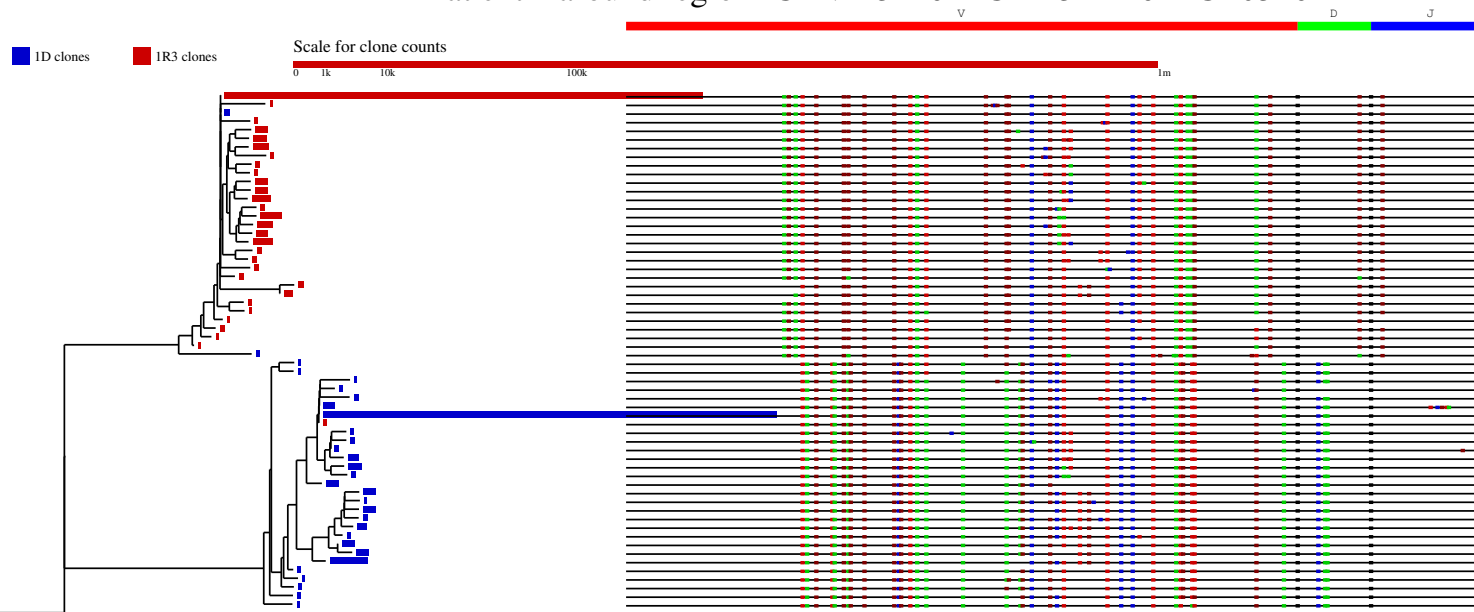
Supplementary Figure 4: Number of the subclones within the dominant VDJ sequence of each sample.

Supplementary Figure 5. Phylogenetic Trees.
A. Pair 1

Patient 1 around region IGHV4-34*02 IGHD3-22*01 IGHJ5*02

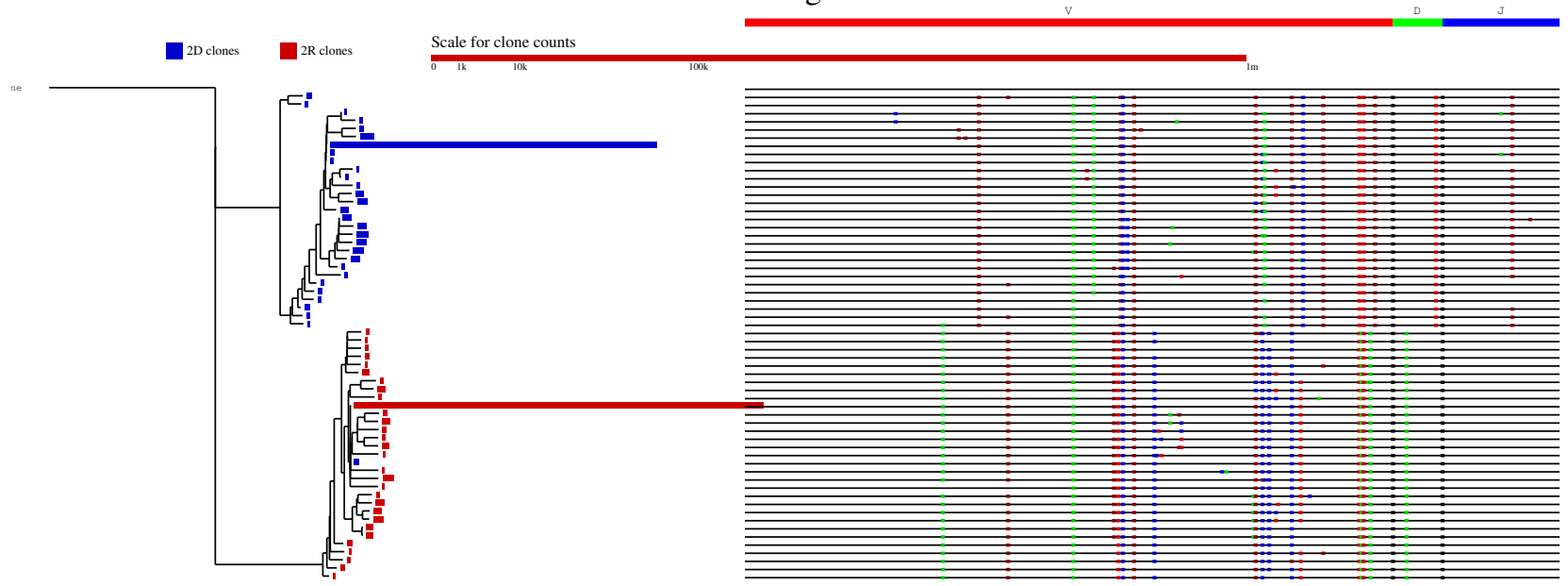


Patient 1 around region IGHV4-34*02 IGHD3-22*01 IGHJ5*02



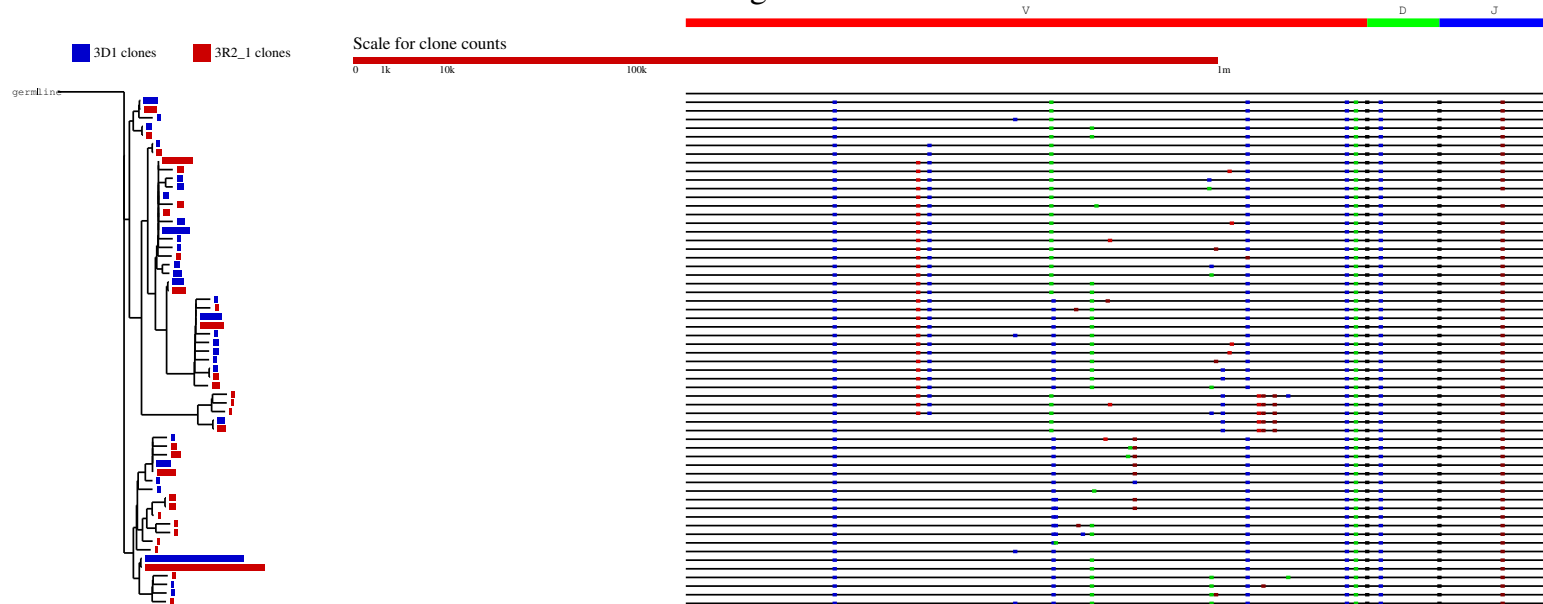
B. Pair 2

Patient 2 around region IGHV4-59*01 IGHD6-19*01 IGHJ5*02

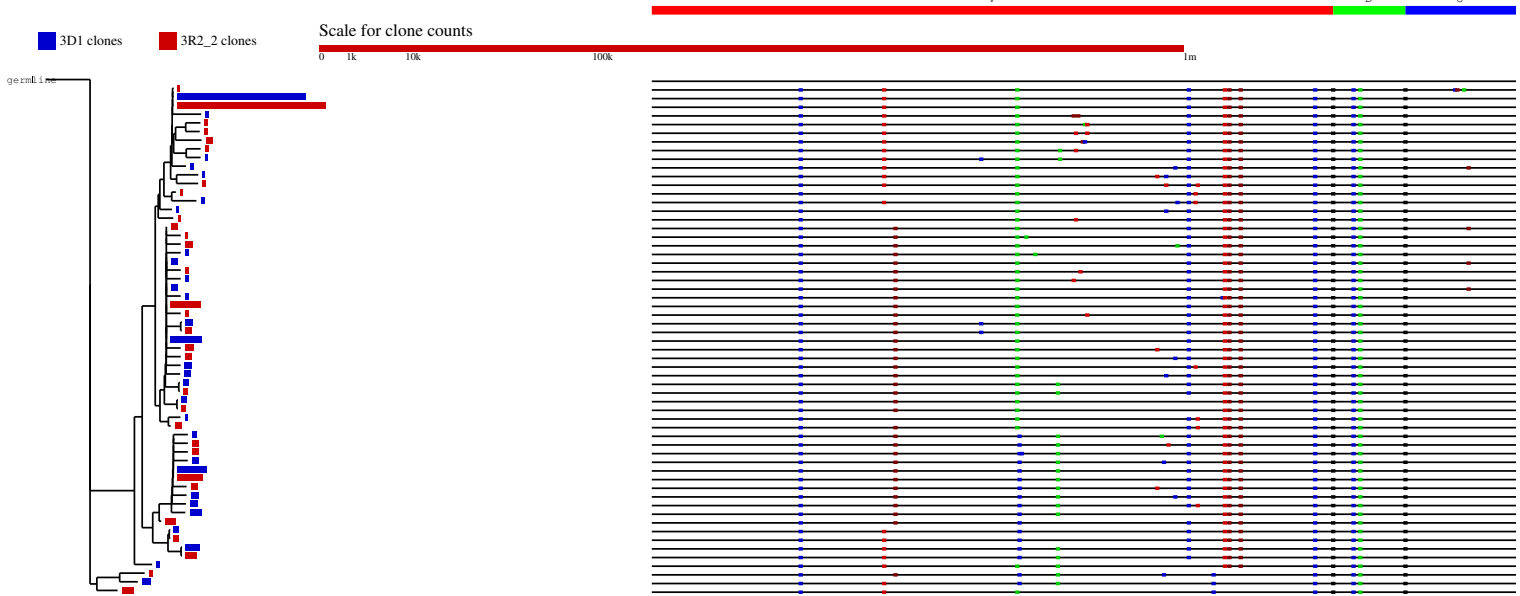


C. Pair 3

Patient 3 around region IGHV3-49*05 IGHD2-8*01 IGHI4*02

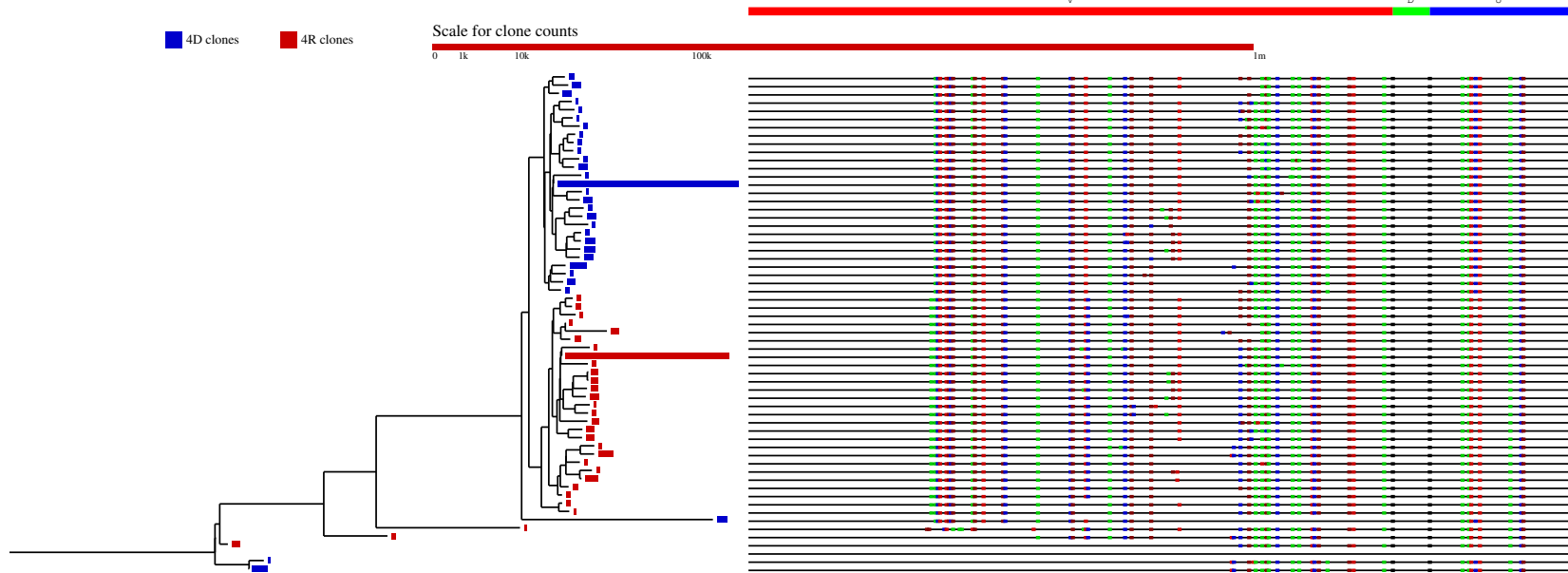


Patient 3 around region IGHV3-49*04 IGHD3-22*01 IGHI4*02



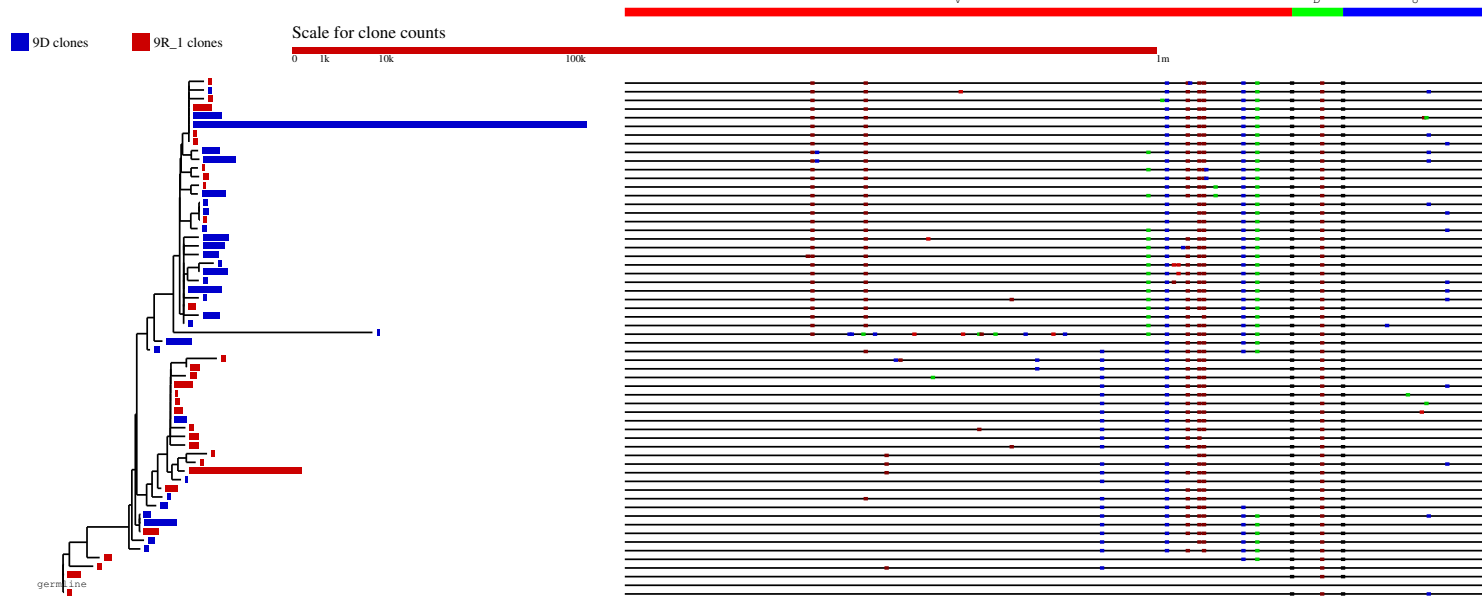
D. Pair 4

Patient 4 around region IGHV3-7*03 IGHD4-17*01 IGHJ6*04



E. Pair 5

Patient 9 around region IGHV4-34*08 IGHD6-13*01 IGHJ6*03

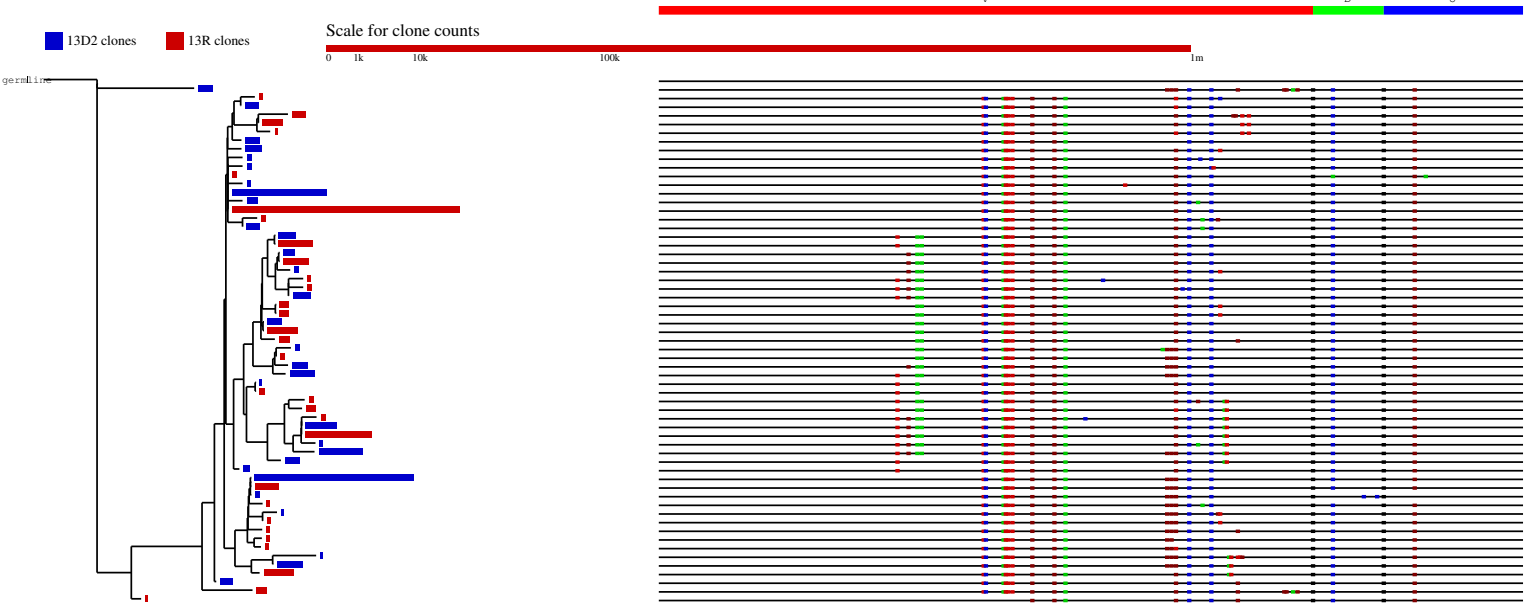


F. Pair 7

Patient 13 around region IGHV3-23*04 IGHD3-9*01 IGHIJ6*02

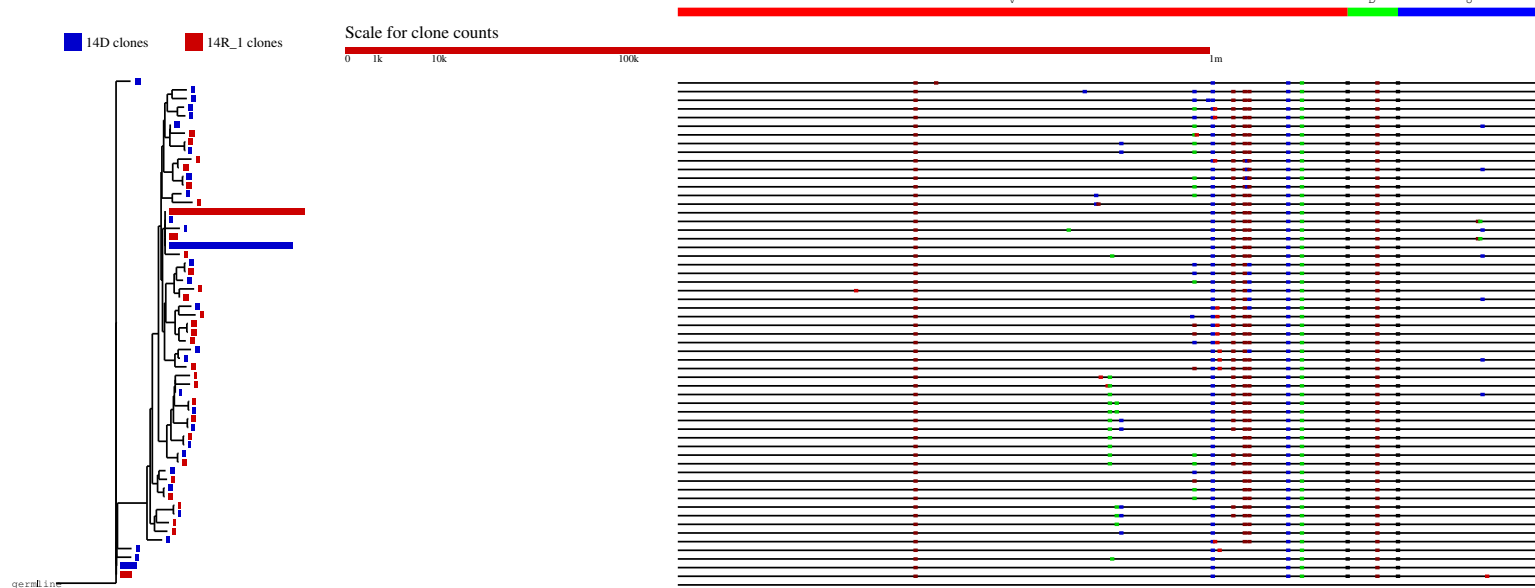


Patient 13 around region IGHV3-23*04 IGHD3-9*01 IGHJ6*02

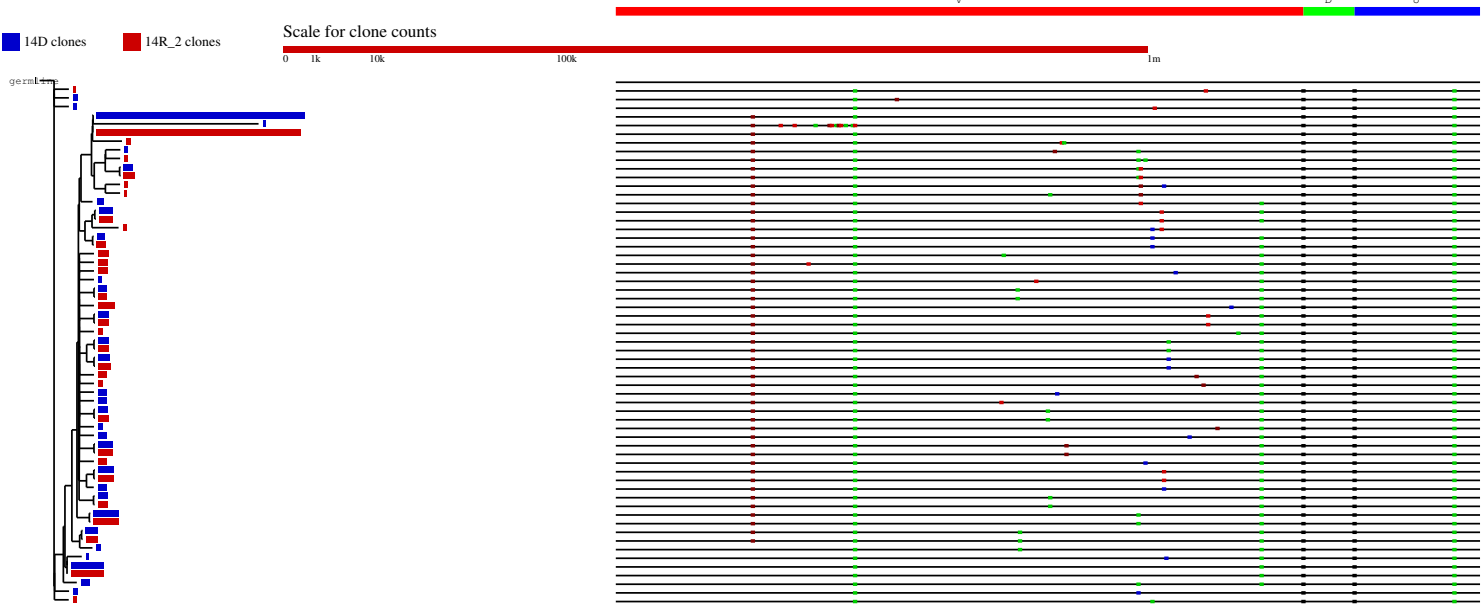


G. Pair 8

Patient 14 around region IGHV4-34*02 IGHD6-13*01 IGHJ6*03

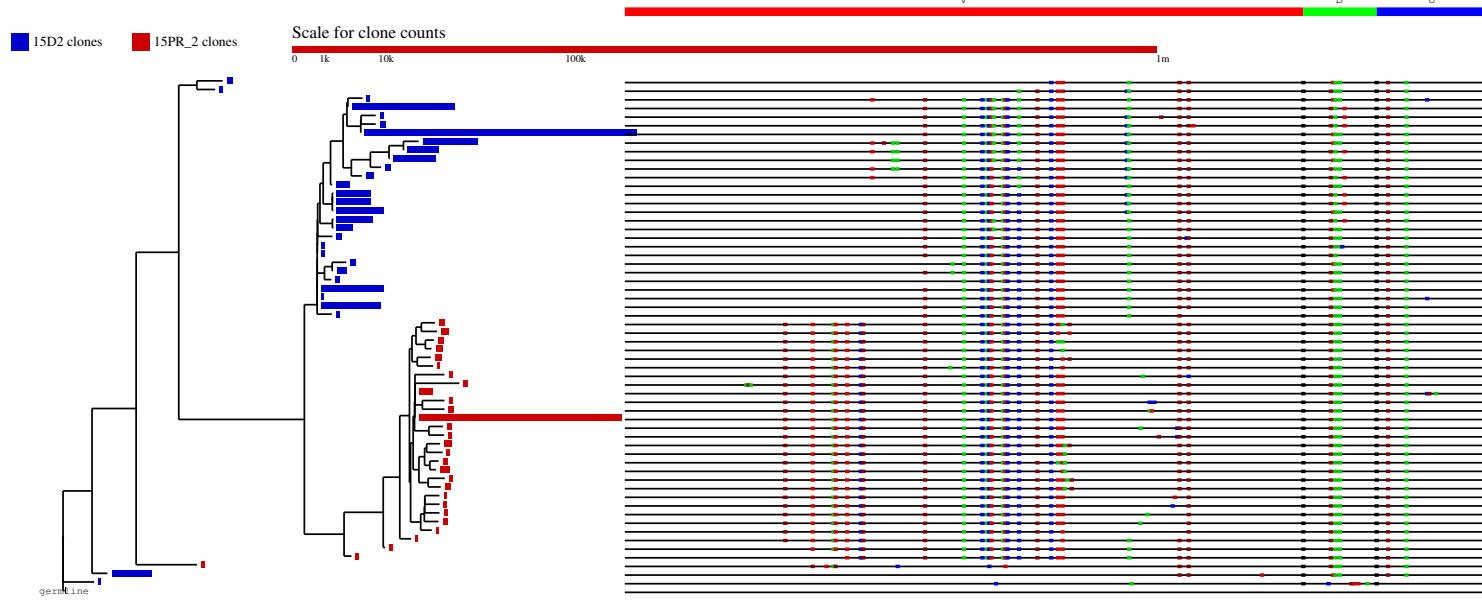


Patient 14 around region IGHV1-18*01 IGHD6-13*01 IGHJ2*01



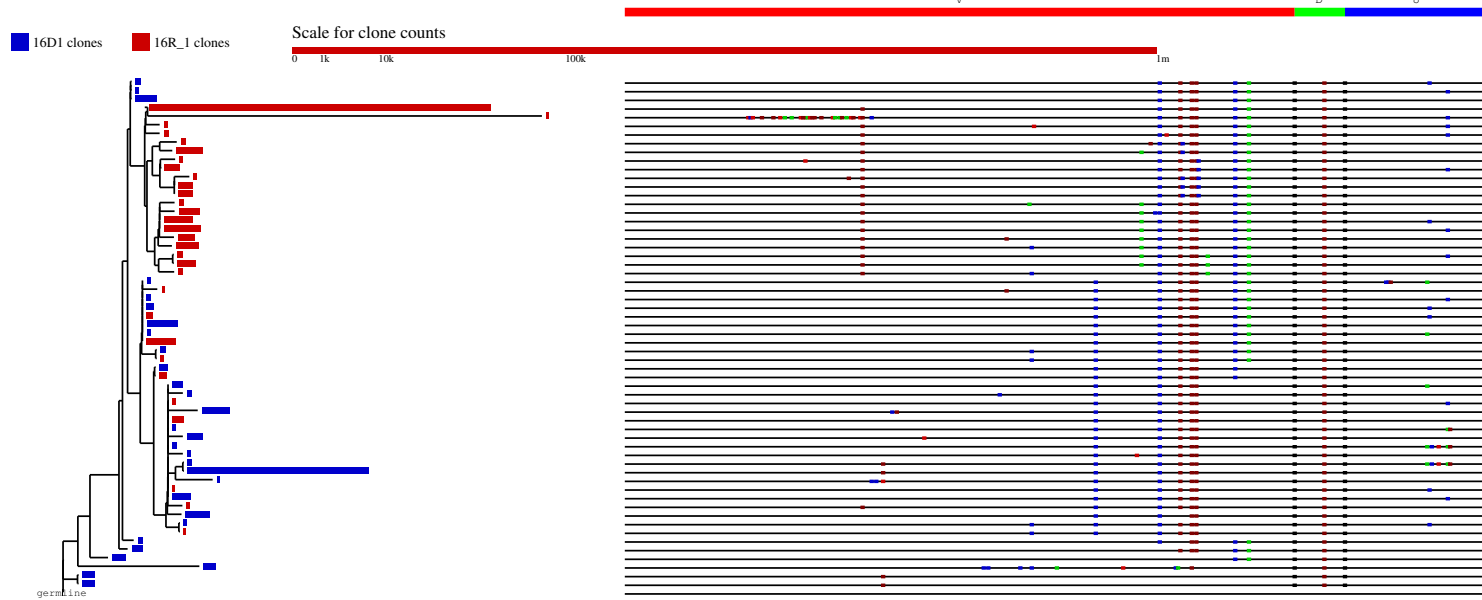
H. Pair 9

Patient 15 around region IGHV3-48*02 IGHD2-2*03 IGHJ4*02



I. Pair 10

Patient 16 around region IGHV4-34*02 IGHD6-13*01 IGHJ6*03



J. Pair 11

Patient F6 around region IGHV3-23*04 IGHD2-15*01 IGHJ4*02

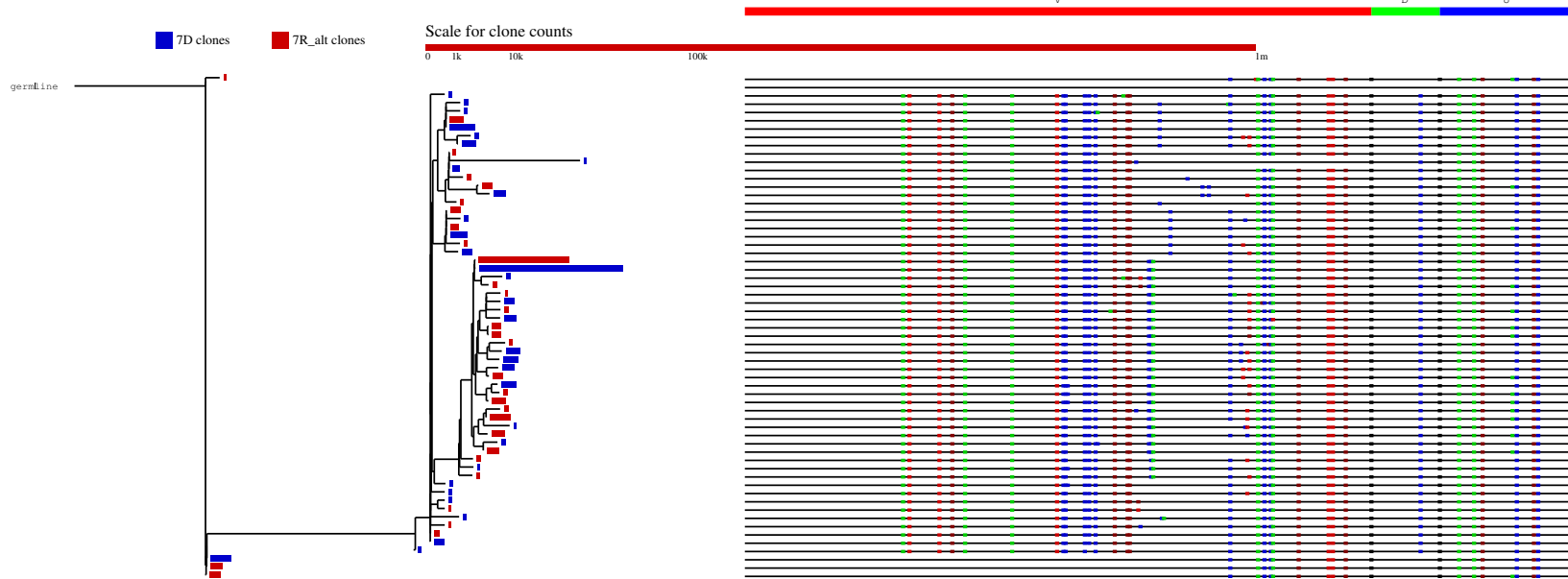


Patient F6 around region IGHV3-23*04 IGHD3-22*01 IGHJ4*02



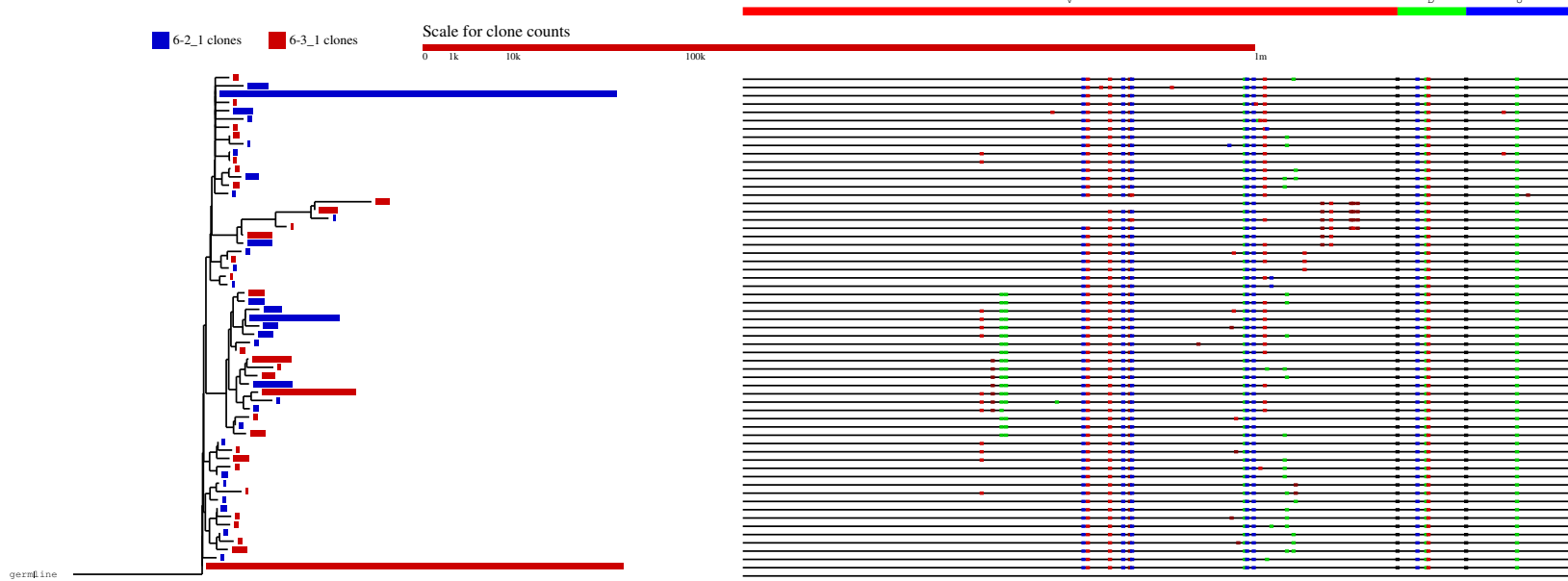
K. Pair 12

Patient F7 around region IGHV4-34*02 IGHD3-22*01 IGHJ6*03

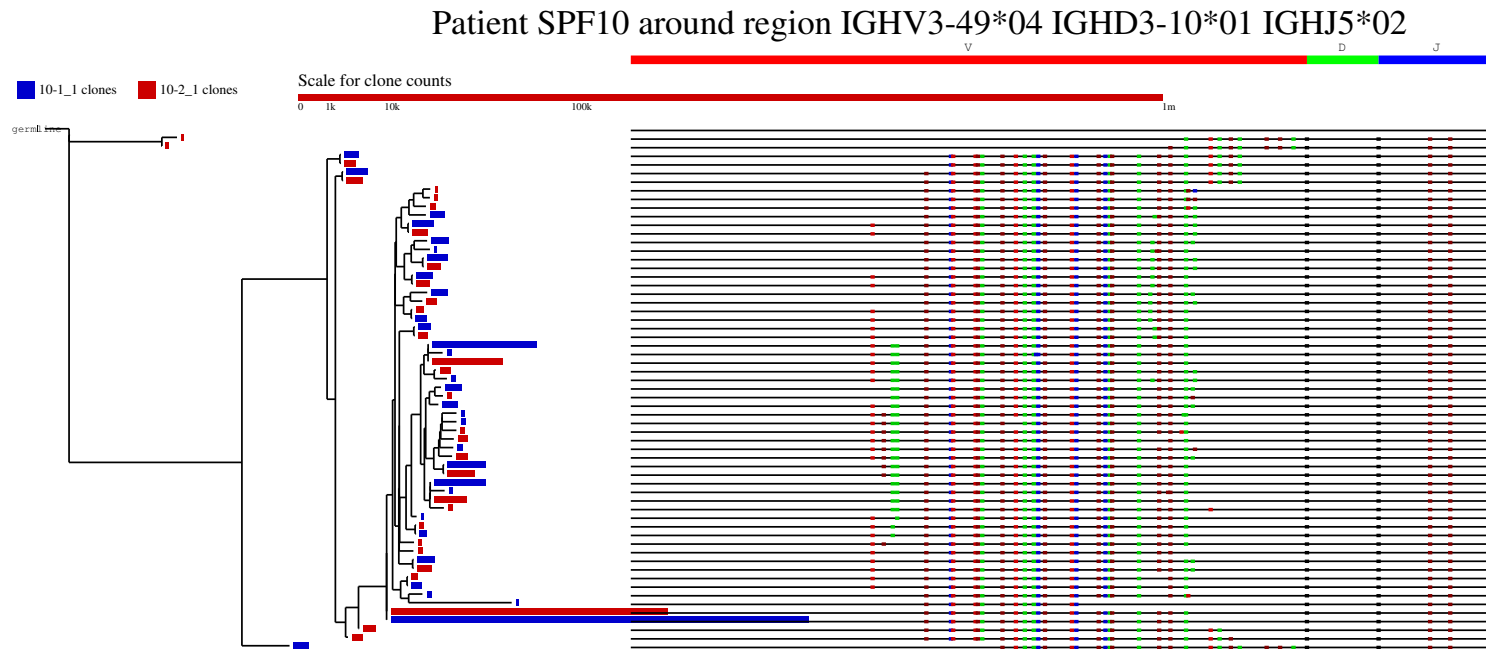


L. Pair 13

Patient SPF6 around region IGHV3-7*03 IGHD3-10*02 IGHJ4*02



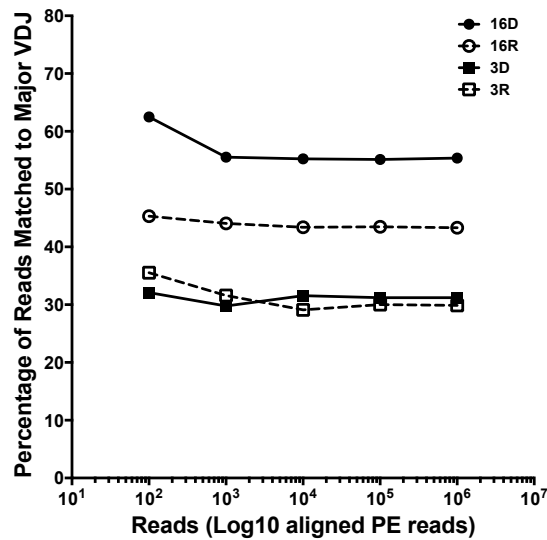
M. Pair 14



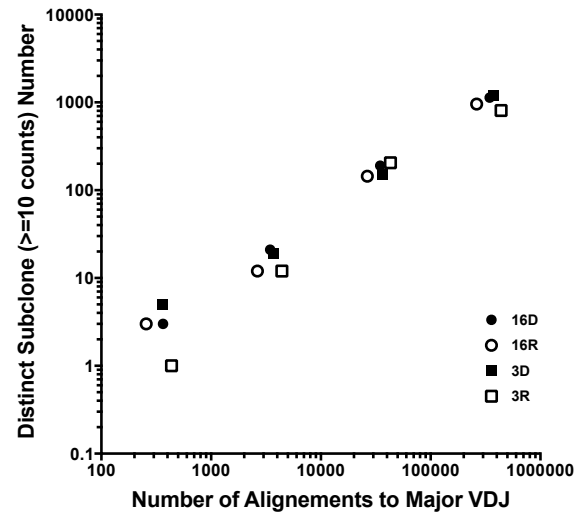
Supplementary Figure 5: Phylogenetic trees for each diagnosis/relapse pair. Phylogenetic analysis of the SHM profiles of the major $V_H D J_H$ rearrangements between each diagnosis and relapse pair was presented in each figure. The blue bar represents the diagnosis rearrangement and the red bar represents the relapse rearrangement. The length of the bar indicates the abundance of the rearrangement.

Supplementary Figure 6

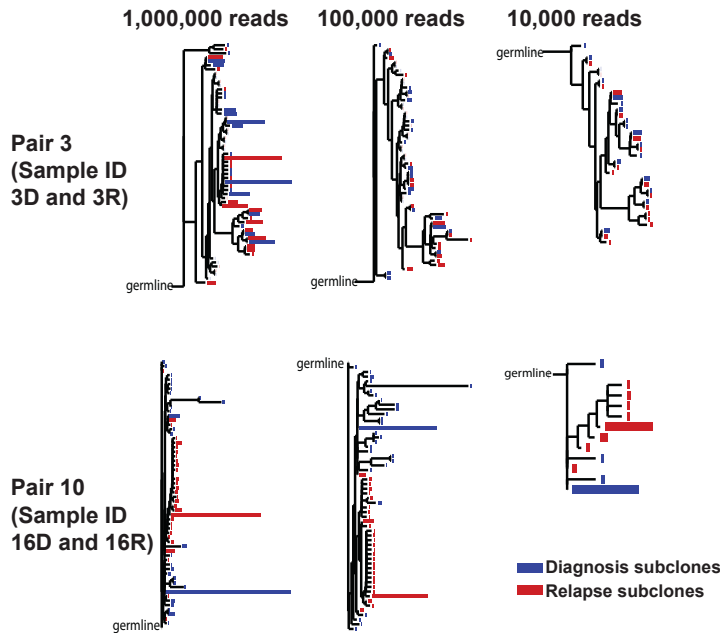
A.



B.



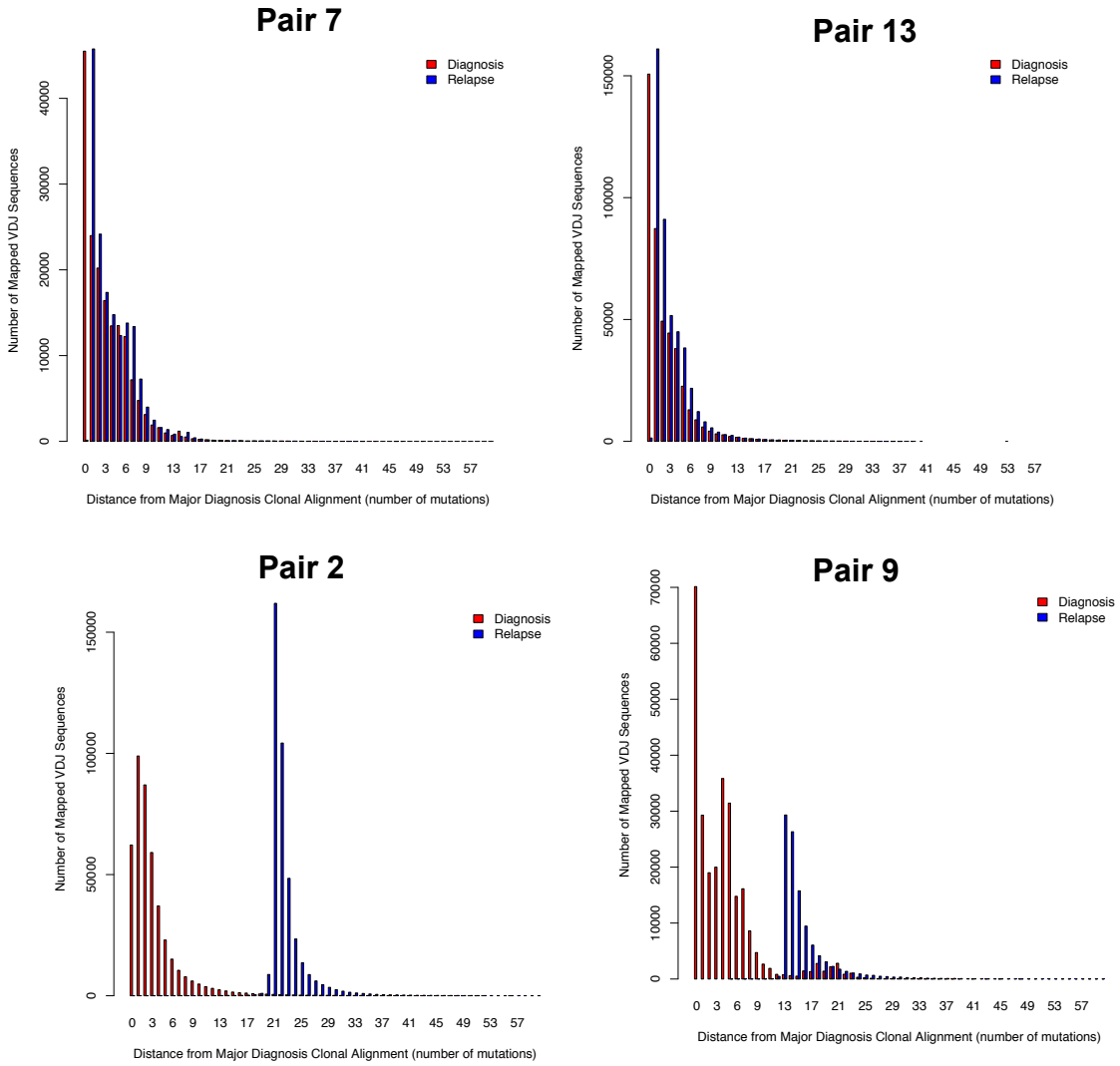
C.



Supplementary Figure 6: Subsampling of VDJ-sequencing. VDJ PCR products of the diagnosis and relapse tumors of pairs 3 (sample ID 3D and 3R) and 10 (sample ID 16D and 16R) were sequenced to roughly 2 million paired reads per sample. The aligned reads were systematically subsampled with decreasing rate to assess the VDJ recombination composition in order to examine: (A). the relationship between the number of reads and the ratio of major VDJ

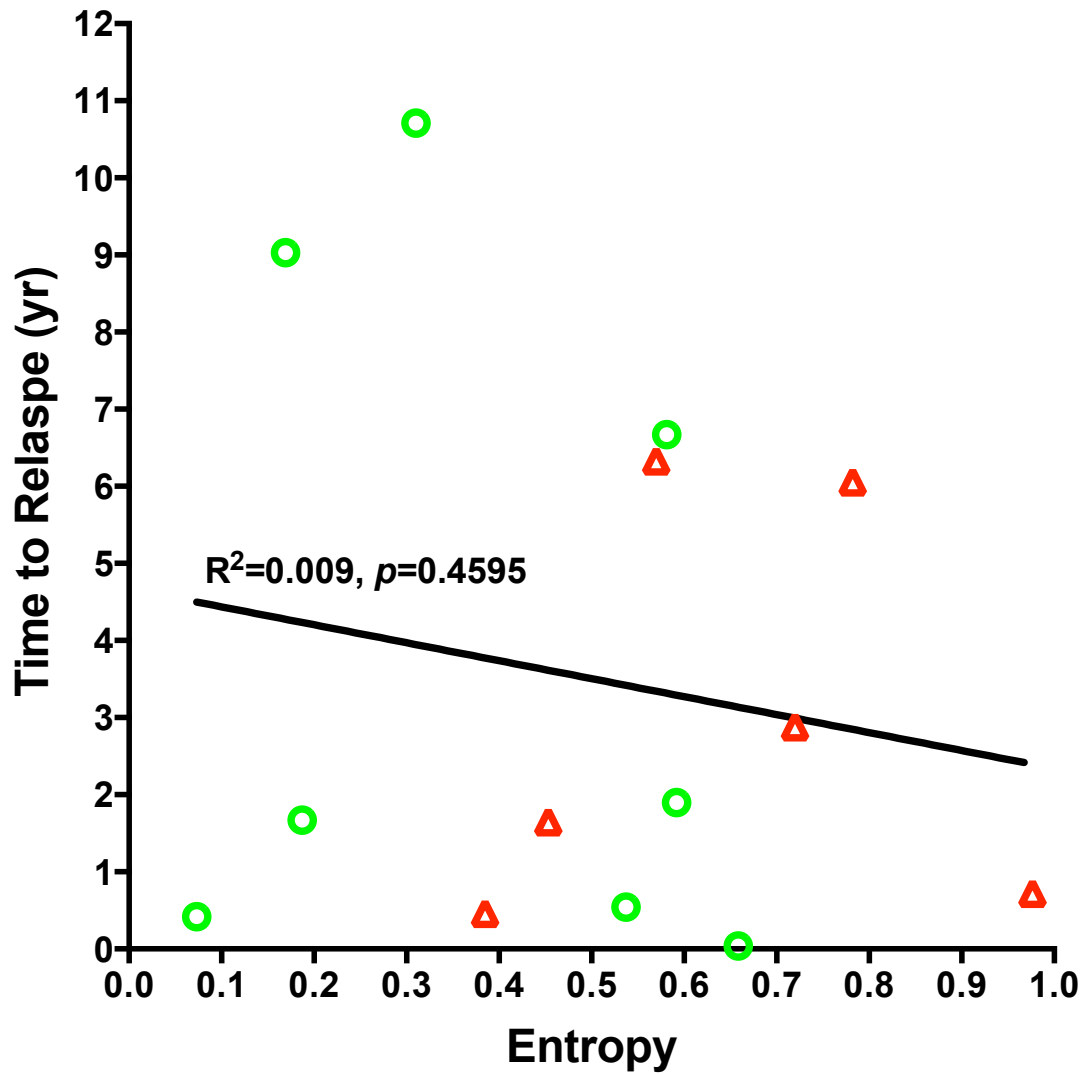
rearrangement; (B). the relationship between the number of aligned reads to major VDJ rearrangement and the number of the subclones within the major VDJ rearrangement; and (C). the phenogenetic trees at different reads number cutoffs.

Supplementary Figure 7:



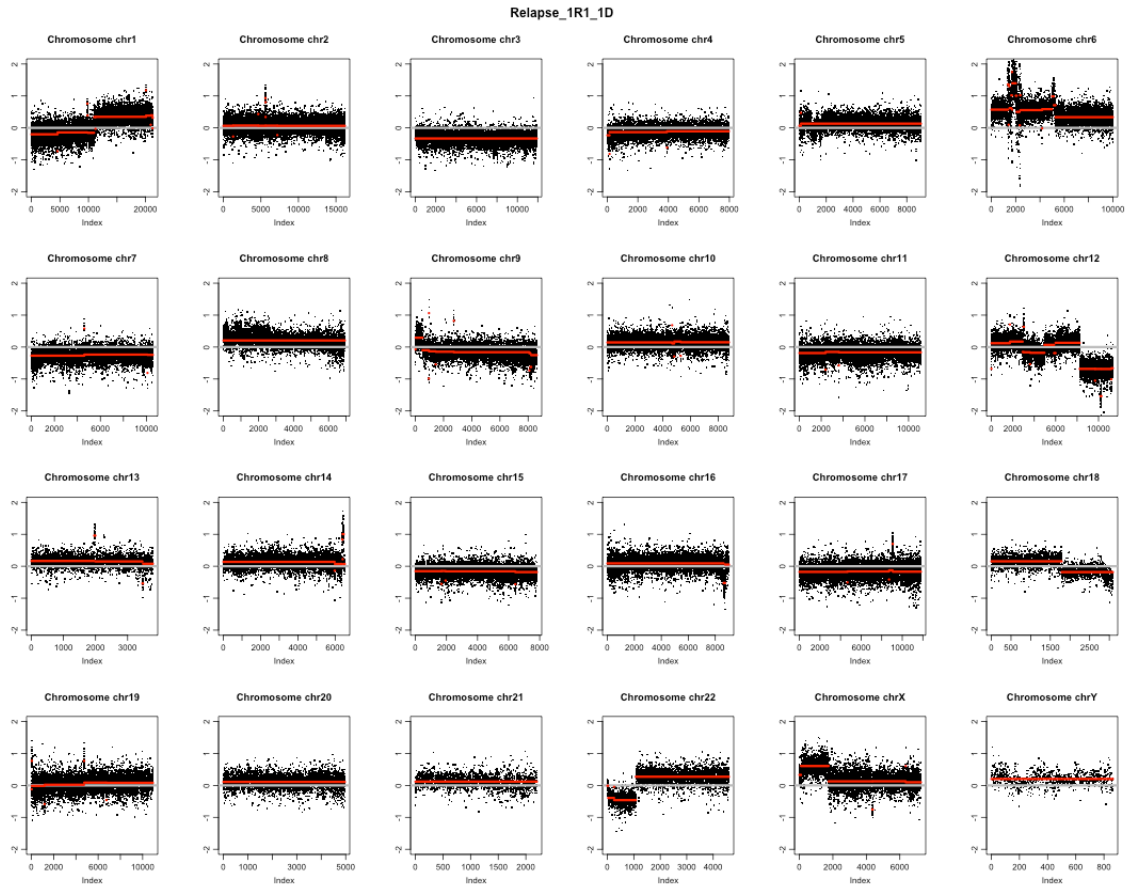
Supplementary Figure 7: Distance of relapse subclones and diagnosis subclones from the major diagnosis subclone. Each bar represents either one diagnosis subclone (red) or relapse subclone (blue). Numbers on X-axis indicate the number of the mutations in that subclone that were different from the major diagnosis subclone.

Supplementary Figure 8

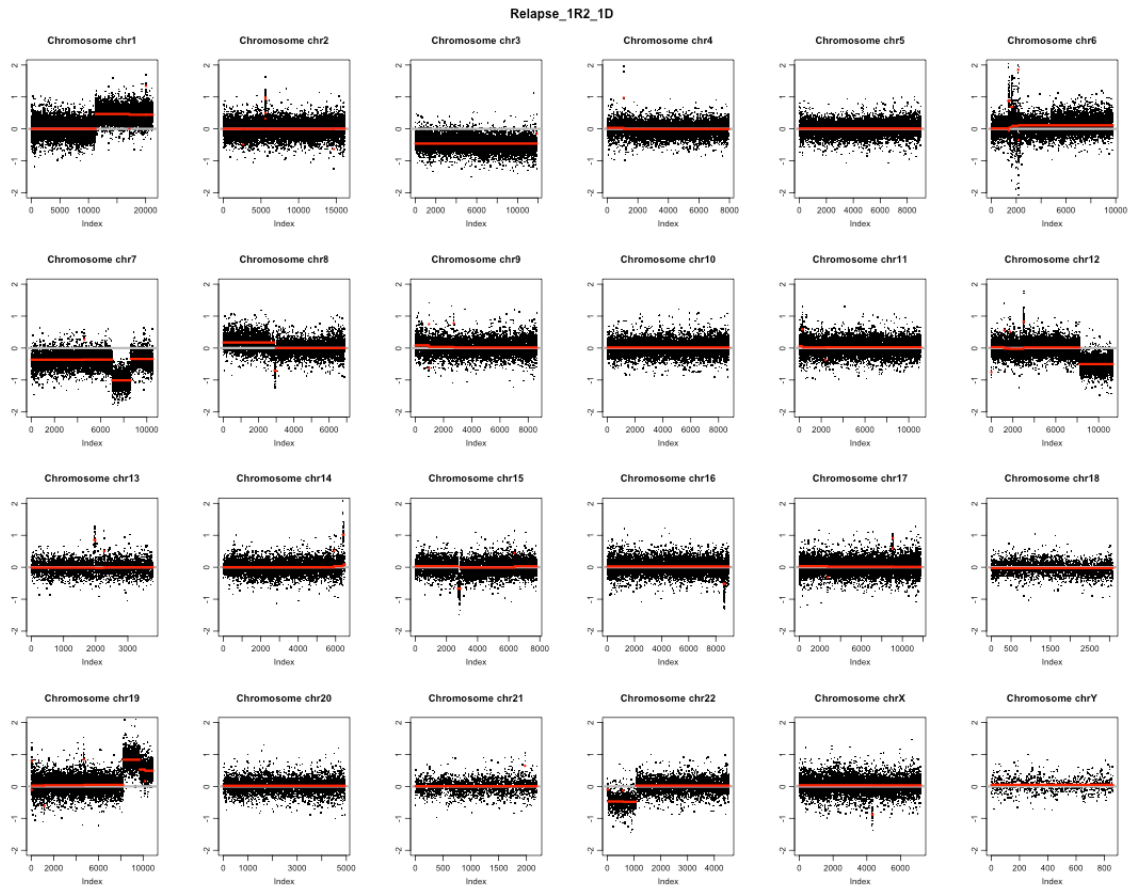


Supplementary Figure 8. The relationship between clonal diversity at diagnosis (measured by entropy) and time to relapse. Red triangles represent diagnosis samples of the early-divergent mode. Green circles represent diagnosis samples of the late-divergent mode.

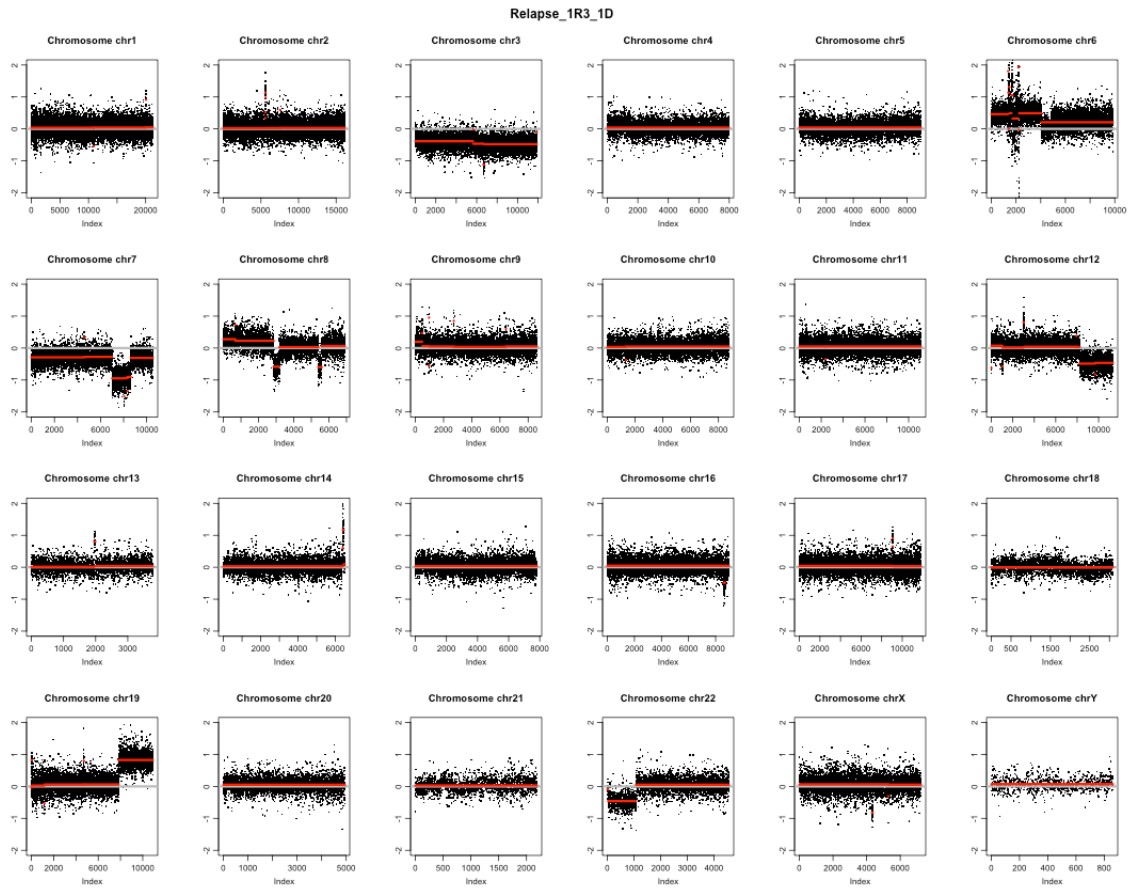
Supplementary Figure 9: CNA plots for each diagnosis/relapse pair.
A: 1R1 vs 1D



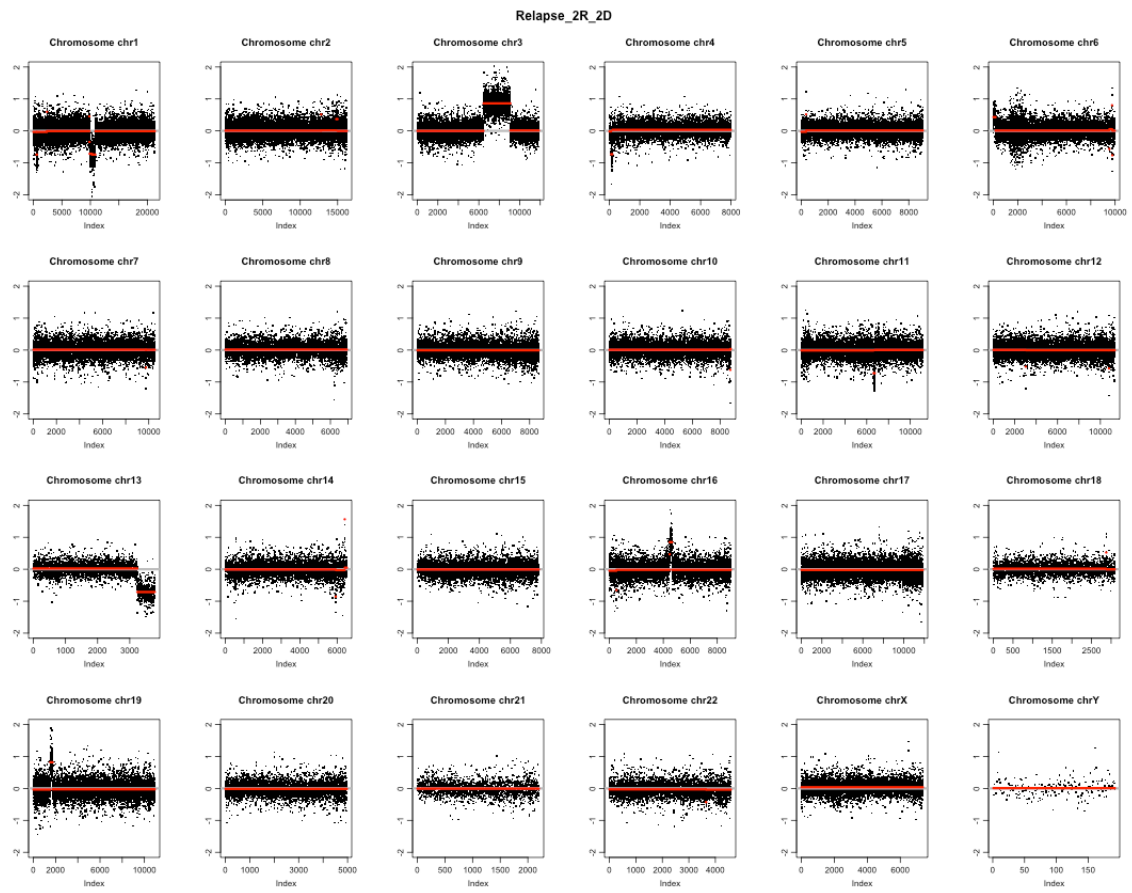
B: 1R2 vs 1D:



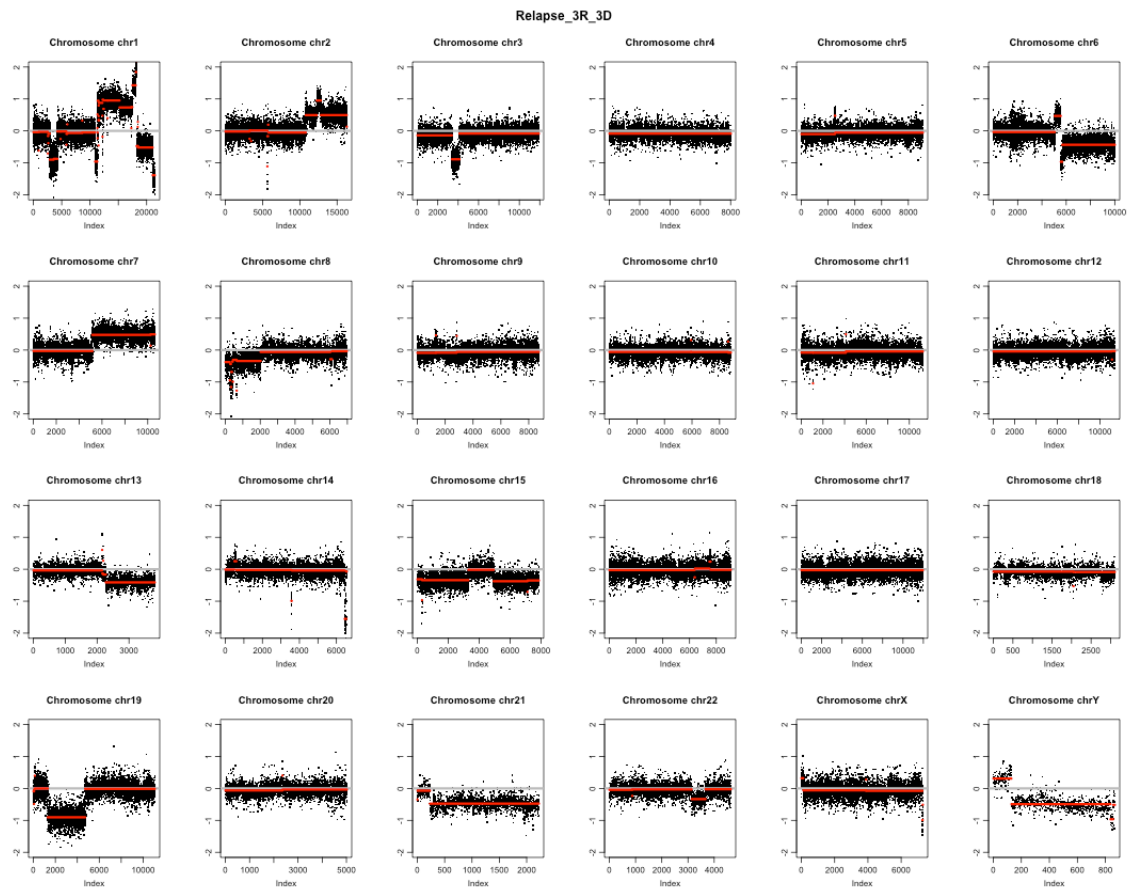
C: 1R3 vs 1D:



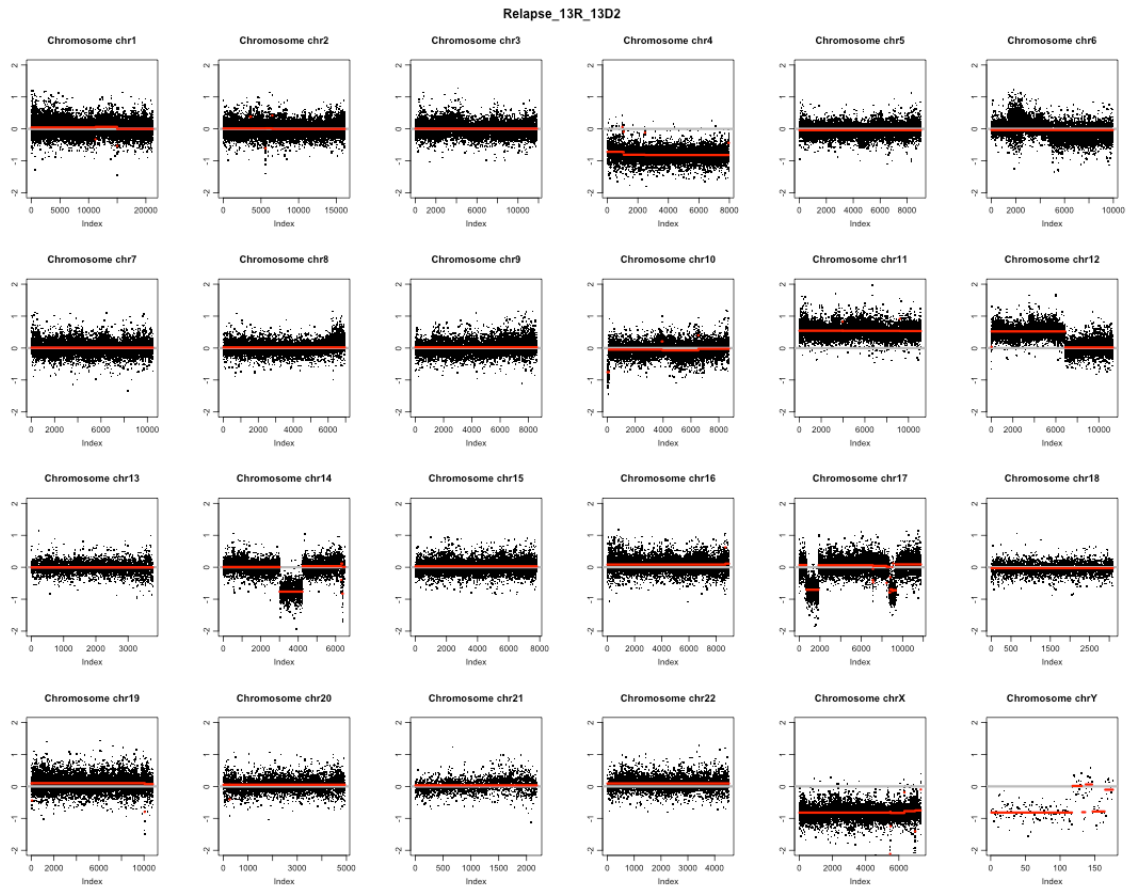
D: 2R vs 2D:



E: 3R vs 3D:

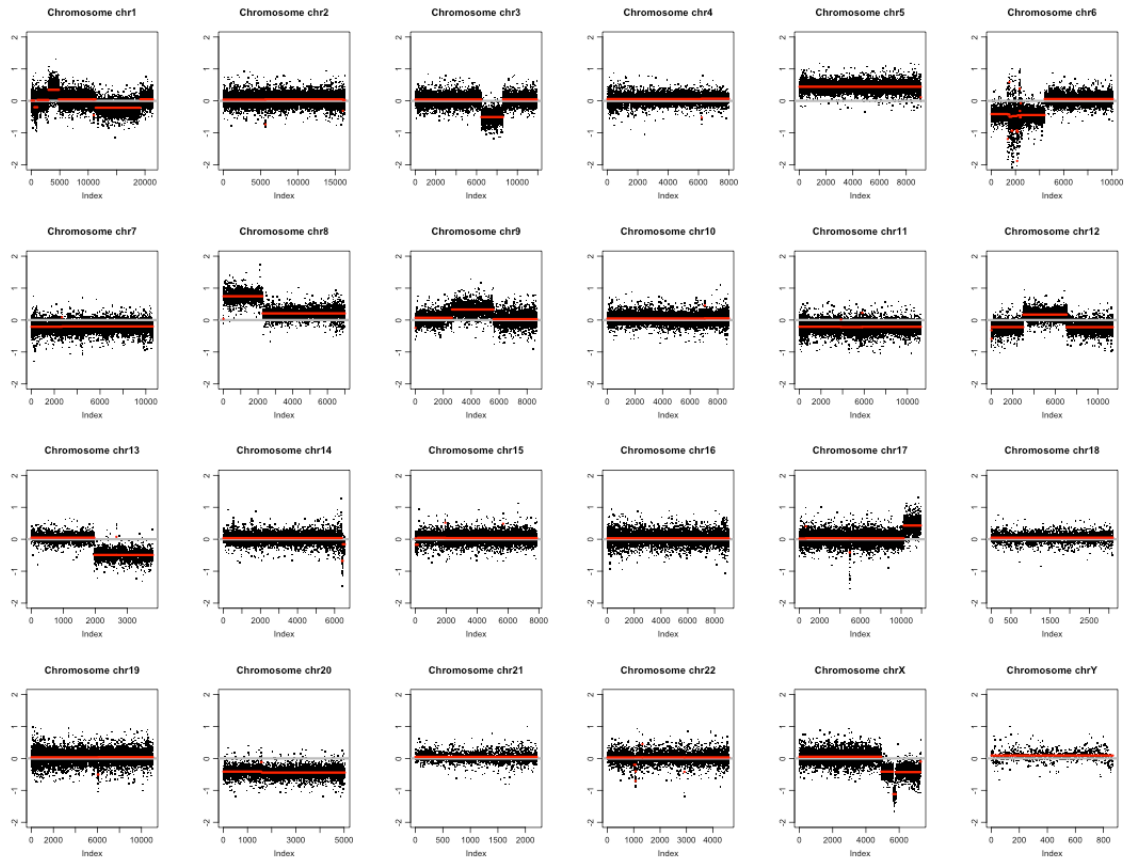


F: 13R vs 13D2:

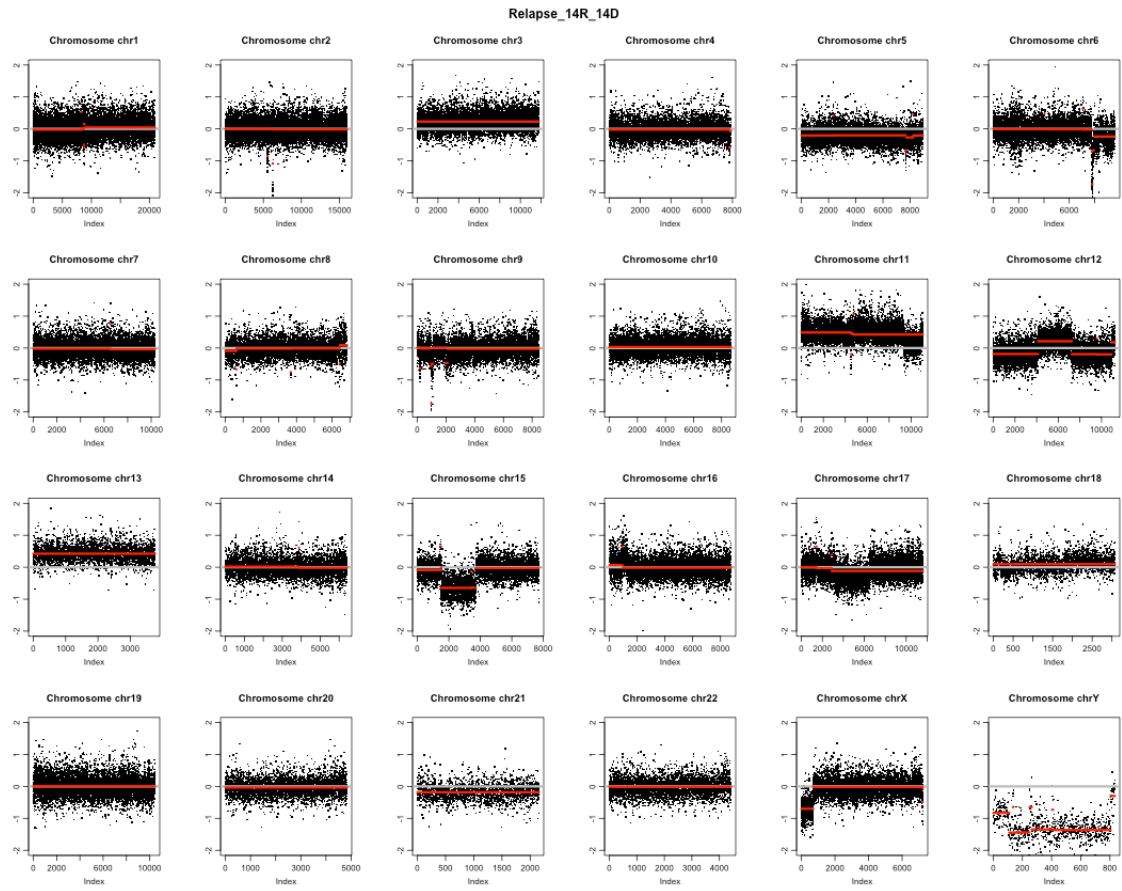


G: 14R vs 14D:

Relapse_14R_14D

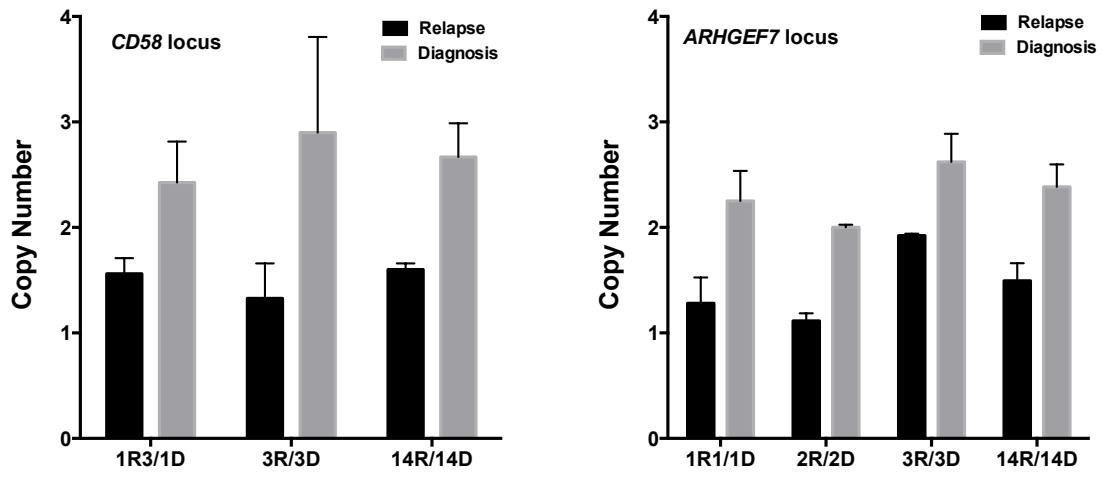


H: 15R vs 15D:



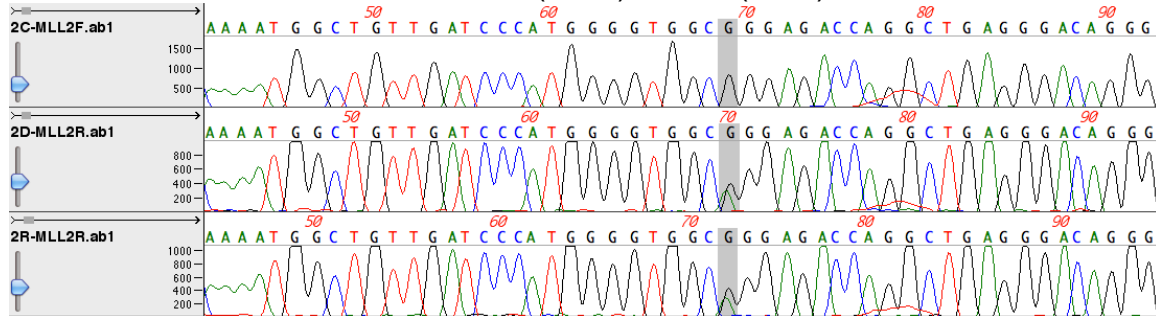
Supplementary Figure 9: CNA plots for each diagnosis/relapse pair. Copy number ratio was calculated between the diagnosis and relapse samples for each exon (represents by black dots, see Methods). The red lines represent the smoothed ratio along each chromosome.

Supplementary Figure 10:



Supplementary Figure 10, copy number validation of the CD58 and ARHGEF7 loci.

Supplementary Figure 11:
2D and 2R, chr12: 49433882, G-> A, (CCG)P2557L(CTG),



Supplementary Figure 11: Sanger sequencing validation of *MLL2* mutation in sample pair 2. Sanger sequencing traces centering around chr12: 49433882 (hg19) were shown for the control DNA sample from liver (top panel), the diagnosis sample (middle panel), and the relapse sample (bottom panel) of patient 2. The shaded area highlights the G to A mutation seen in the diagnosis and relapse samples, but not in the normal control sample.